1 Kaneko's Model of Electronic Stopping

The Stopping cross section per target atom is the sum of the independent contributions of its shells with individual occupation numbers N_{sh}

$$-\frac{dE}{dx} = S\rho_{\text{at}} \quad ; \quad S = \sum_{\text{sh=bnd,free}} S_{\text{sh}} \quad ; \quad \sum_{\text{sh=bnd,free}} N_{\text{sh}} = Z_2 . \tag{1}$$

Polarization charges ρ_p are excited in each shell

$$\rho_p(\vec{k}, \omega) = \rho_m(\vec{k}, \omega) \left[\frac{1}{\epsilon_{\text{sh}}(\vec{k}, \omega)} - 1 \right],$$

where

$$\rho_m(r) = Z_1 e \delta(r) + \rho_e(r) \tag{2}$$

means the ion charge density in its rest frame and $\rho_m(k)$ its Fourier transform (form factor). $\rho_e(r)$ is the radial charge distribution of the N bound electrons. Results presented here insert the Brandt-Kitagawa ion model

$$\rho_e(r) = -e \frac{N}{4\pi\Lambda^2} \frac{\exp(-r/\Lambda)}{r},$$

and borrow the size parameter Λ and $N(v)$ from the Ziegler-Biersack-Littmark (ZBL) program. In solid targets and if appropriate, the stopping cross section of some N_{free} electrons of the outermost target shell is described by the Lindhard-Winther theory.

The ground state of the inner shells of bound target electrons is approximated by wave packets with Gaussian momentum distributions

$$w(p) \propto \exp\{-(p/\bar{q}_{\text{bnd}})^2\}. \tag{3}$$

The characteristic wave numbers $\bar{q}_{\text{bnd}}(Z_2)$ are derived from Roothaan-Hartree-Fock calculations of free target atoms.

The susceptibility χ^R of each atomic shell is computed in a random phase approximation

$$\chi^R_{\text{bnd}}(k,\omega) = \frac{e^2}{4\pi^3\hbar k^2\epsilon_0}\int d^3p \frac{w(\vec{p}+\vec{k}) - w(\vec{p})}{\omega - \hbar(\vec{p}+\vec{k})^2/(2m) + \hbar\vec{p}^2/(2m) + i\eta}. \tag{4}$$

$$\epsilon_{\text{sh}}(k,\omega) = 1 + \chi^R_{\text{sh}}(k,\omega).$$

Stopping cross section of inner target shells with N_{bnd} electrons:

$$S_{\text{bnd}} = -\frac{2}{\sqrt{\pi}\epsilon_0 v^2}\frac{N_{\text{bnd}}}{\bar{q}^3_{\text{bnd}}}\int_0^\infty \frac{dk}{k}\,|\rho_m(k)|^2\int_0^{kv}\omega\Im\left[\frac{1}{\epsilon_{\text{bnd}}(k,\omega)} - 1\right]d\omega. \tag{5}$$

- general ion velocities v; general elemental targets Z_2 in “random” direction
- real and imaginary parts of $\chi^R_{\text{sh}}(k,\omega)$ in terms of Kummer’s Functions and exponentials
- parameter-free theory if ions are bare

2 Enforcing Band Gaps for Excitations of Inner Target Shells

Eq. (4) allows unrestricted energy or momentum transfer to target electrons. We set

$$\Im\epsilon_{\text{bnd}}(k,\omega) = 0 \quad \text{if} \quad |\ \hbar\omega| < E_g, \tag{6}$$

where E_g is the gap between the orbital energy of the target subshell and the highest occupied atomic level. This strictly excludes electron excitation into band gaps. ϵ_{free} is not modified.

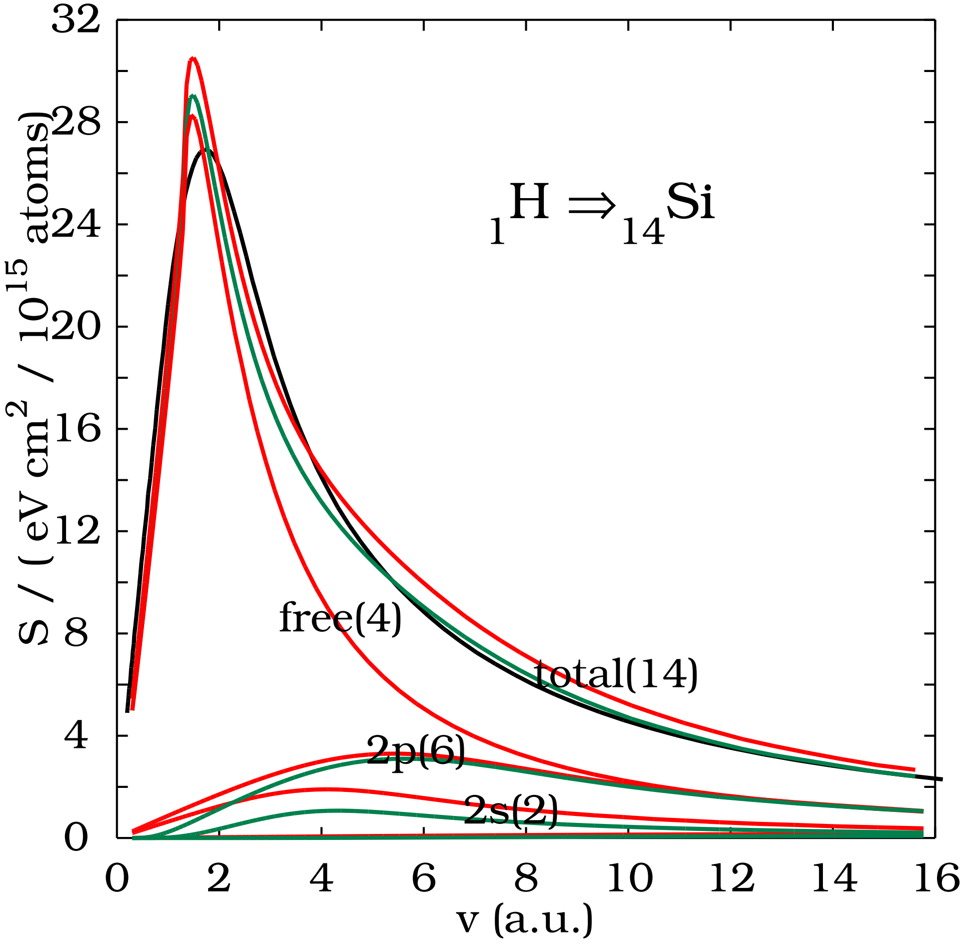

Schematic for e. g. the $_{14}$Si target:

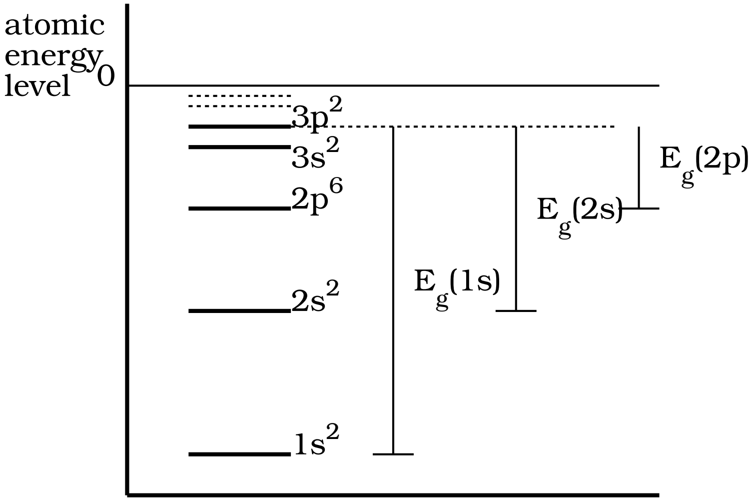

original theory; with energy cut ; ZBL;
Paul-Semrad-Seilinger or Eppacher-Semrad

The high velocity electronic stopping of protons then coincides with the experimental data. The remaining under-estimation at small velocities is a known artifact of the RPA.

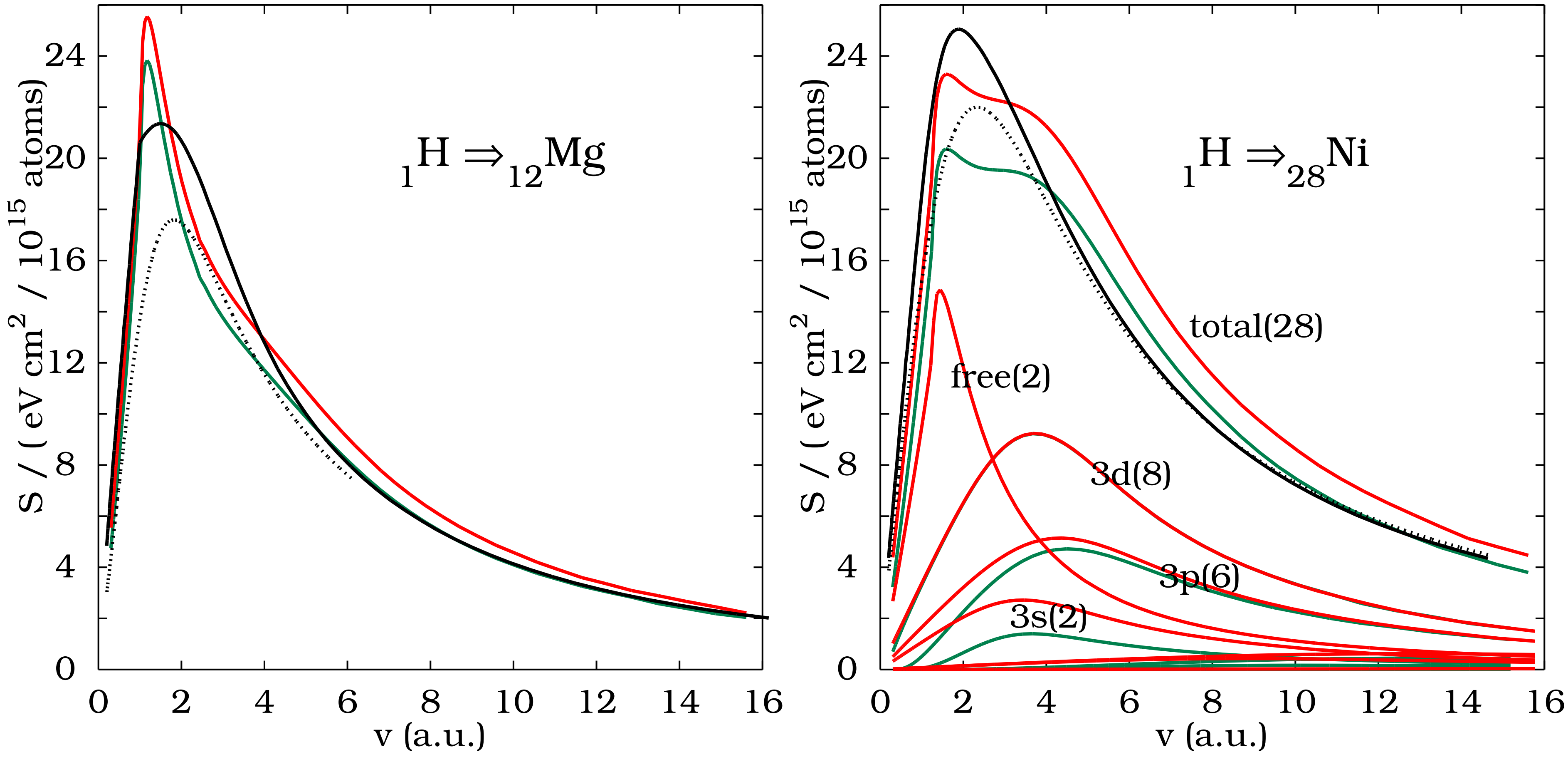

4 Mutual (Anti)Screening between Polarization Charges of Different Target Shells

The independent excitations in (1) should be replaced by defining *one* joint "macroscopic" dielectric function

$$\epsilon = 1 + \sum_{\text{sh=bnd,free}} \frac{\rho_{\text{at}}}{\rho_{\text{sh}}} \chi^R_{\text{sh}}(k, \omega)$$

in order to add susceptibilities, not polarization charges. It means, the Kaneko susceptibilities with densities $\rho_{\text{sh}} \propto \bar{q}^3$ of closely packed target shells are first diluted to the actual density ρ_{at}. Then the excitation of each shell is determined by the joint field of the ion and the polarization charges of the remaining shells. Thus, a Hartree interaction between the polarization charges of different shells is switched on.

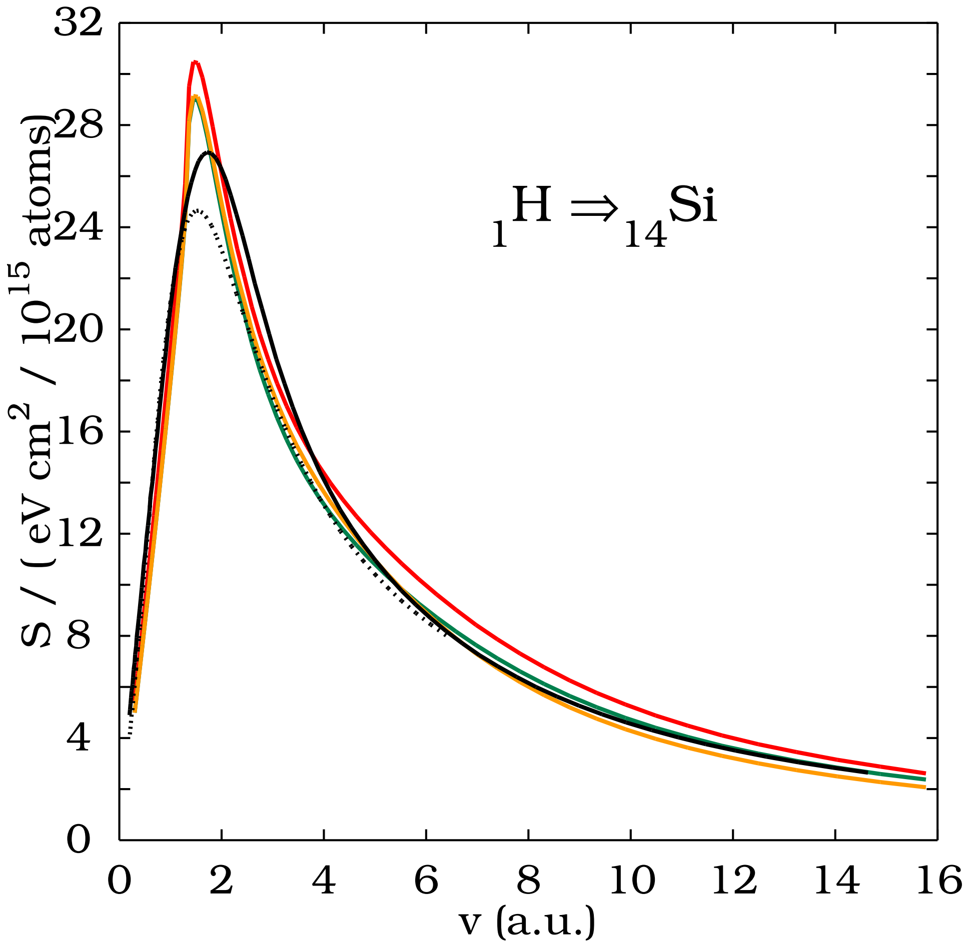

$$\frac{dE}{dx} = \frac{1}{2\pi^2 \epsilon_0 v^2} \int_0^\infty \frac{dk}{k} |\rho_m(k)|^2 \int_0^{kv} \omega \Im \left[\frac{1}{\epsilon(k, \omega)} - 1 \right] d\omega.$$

original theory; with energy cut and dead sphere;
energy cut, dead sphere (r_c in units of Λ) plus joint χ^R; ZBL

This procedure mainly affects the case of transition metal targets. Their free and 3d electrons are "closely coupled" by this overlay of excitation spectra. Their free-electron plasmons get generally damped by the simultaneous occurrence of the 3d single particle "decay channel."

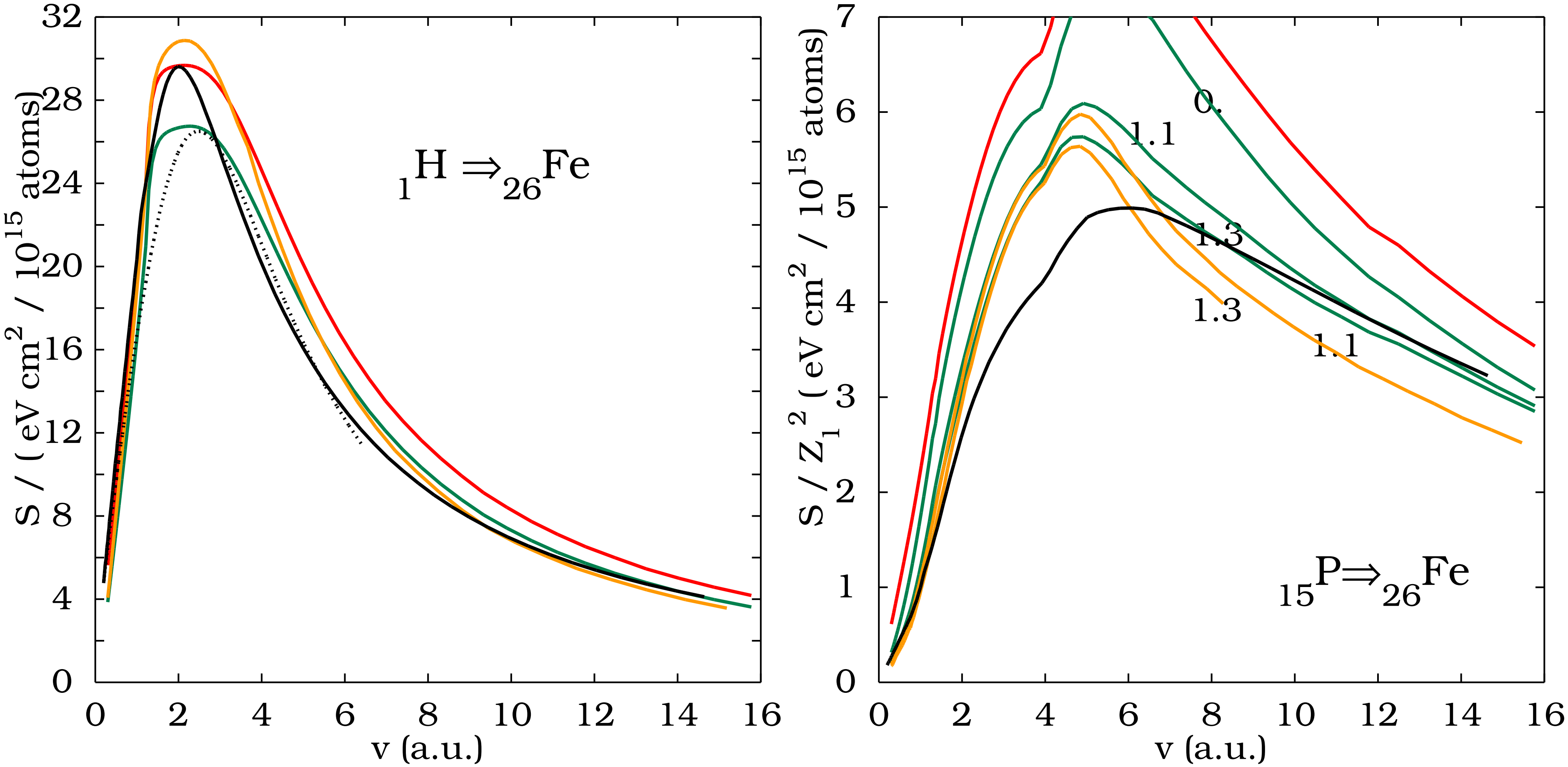

3 Deletion of Polarization Charges at Places within Heavy Ions

Eq. (5) and the Lindhard-Winther theory assume the creation of polarization charges ρ_p at any place,

$$-\frac{dE}{dx} = \vec{v} \int \rho_m(\vec{r}) \vec{\nabla}_r \Phi_{\text{ind}}(\vec{r}) d^3r.$$

We set ρ_p to zero inside a "dead sphere" with radius r_c around the ion nucleus to take into account that the inner shells of heavy ions prevent target electrons to be accumulated or detached from there. In terms of fact we rewrite the electrical potential Φ_{ind},

$$\Phi_{\text{ind}}(\vec{r}, t) = \frac{1}{4\pi\epsilon_0} \int_{|\vec{r}\,' - \vec{v}t| > r_c} \frac{\rho_p(\vec{r}\,', t)}{|\vec{r} - \vec{r}\,'|} d^3r'.$$

The dead sphere leads also to an important reduction of the Stark-energy $\propto \int \rho_n(\vec{r}) \Phi_{\text{ind}}(\vec{r}) d^3r$ that contributes to the ionization degree.

In the two figures below curves are labeled with the frozen radii r_c of the dead spheres, which is ./. for $r_c = 0$, or K, L or M to indicate sizes according to the corresponding ion shell radius. Light ions approximately up to $_5$B are best modeled without dead sphere.

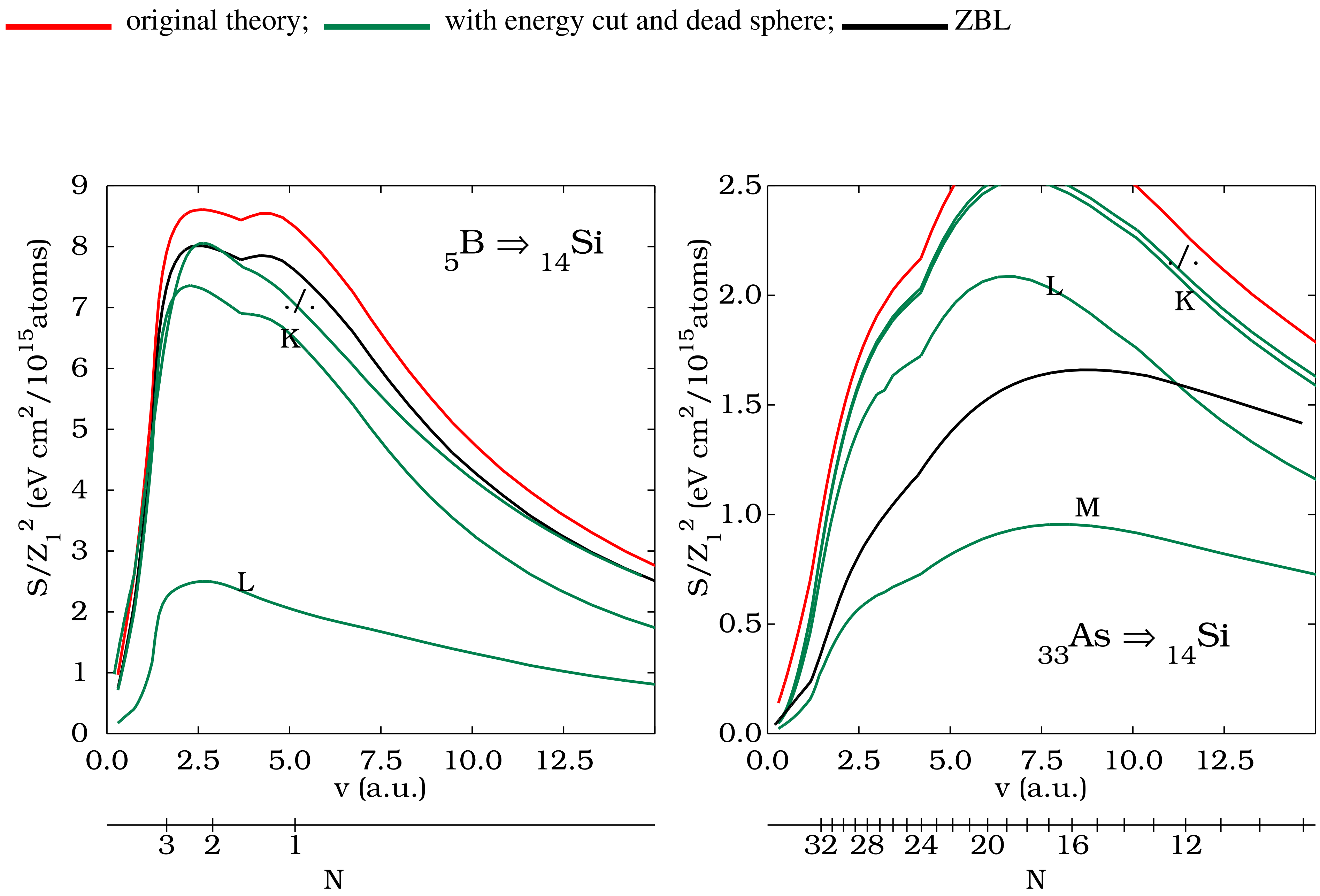

original theory;
with energy cut and dead sphere;
ZBL
$_{5}B \Rightarrow {}_{14}Si$
S/Z_1^2 (eV cm^2/10^{15}atoms)
v (a.u.)
N
K
L
$_{33}As \Rightarrow {}_{14}Si$
M

Below, to the left and right, the dead sphere radius is given in units of Λ (= fractional numbers at curves). It is supposed to shrink with Λ "dynamically" as v increases and the number N of bound electrons decreases.

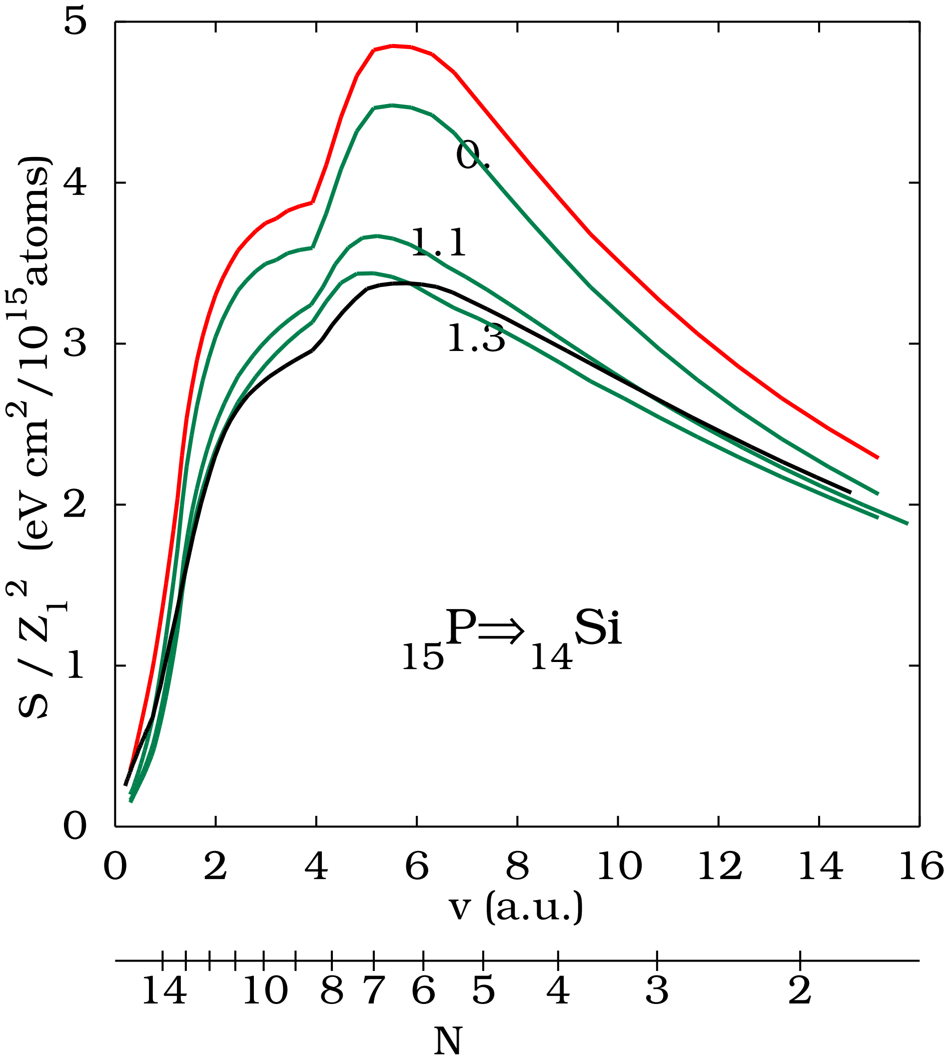

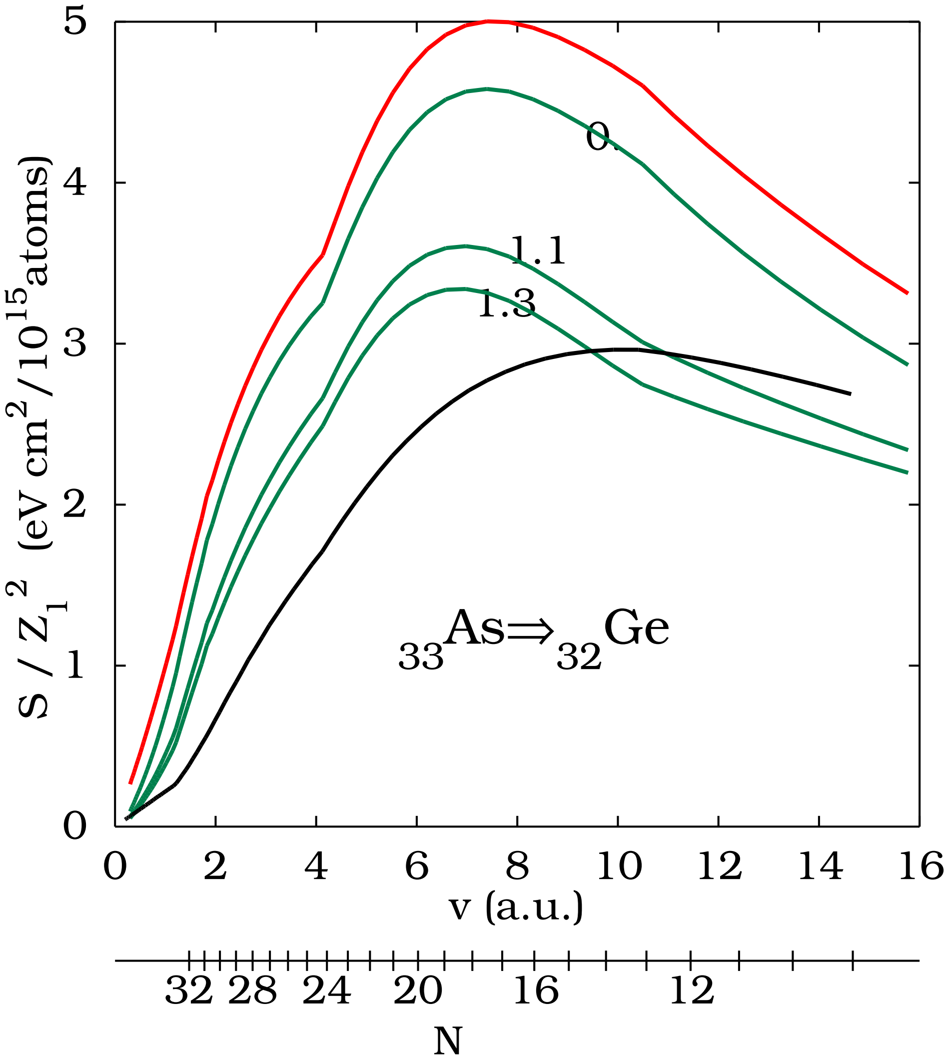

5 New Momentum Distributions of Ground States of Inner Target Shells

Eq. (3) is a good approximation, if the wave functions $\varphi_{\text{bnd}}(\vec{r})$ of the target atom shells are averaged over $\hat{\vec{r}}$ prior to the construction of the wave packets by a Fourier transformation. Our more accurate ansatz first builds the wave packets $\varphi_{\text{bnd}}(\vec{p})$ and averages later on over $\hat{\vec{p}}$, the directions of the wave numbers $\vec{p}$. The generalized fit reads:

$$w(p) \propto p^{2l} \exp\{-(p/\bar{q}_{\text{bnd}})^2\}, \tag{7}$$

with l the angular momentum quantum number of the target subshell. Shells with $l = 0$ (s-shells) or free electrons are not modified. The prefactors are determined by the conservation of the total number N_{bnd} of electrons, and the new characteristic momenta from a comparison with atomic wave functions.

The effect on the energy loss functions of the p- and d-shells is comparatively small. The maximum of the stopping powers of these sub-shells is shifted towards higher ion velocities. The ZBL ionization degree and size parameter merged into the ion form factor ρ_m of the Kaneko theory do not keep the maxima of heavy ions in line with the "pure" ZBL results.

The figures below display results of mixtures of the four changes proposed here.

original theory; with energy cut and dead sphere;
energy cut, dead sphere plus joint χ^R; ZBL
energy cut, dead sphere and non-Gaussian momentum distributions;
energy cut, dead sphere, non-Gaussian momentum distributions and joint χ^R;

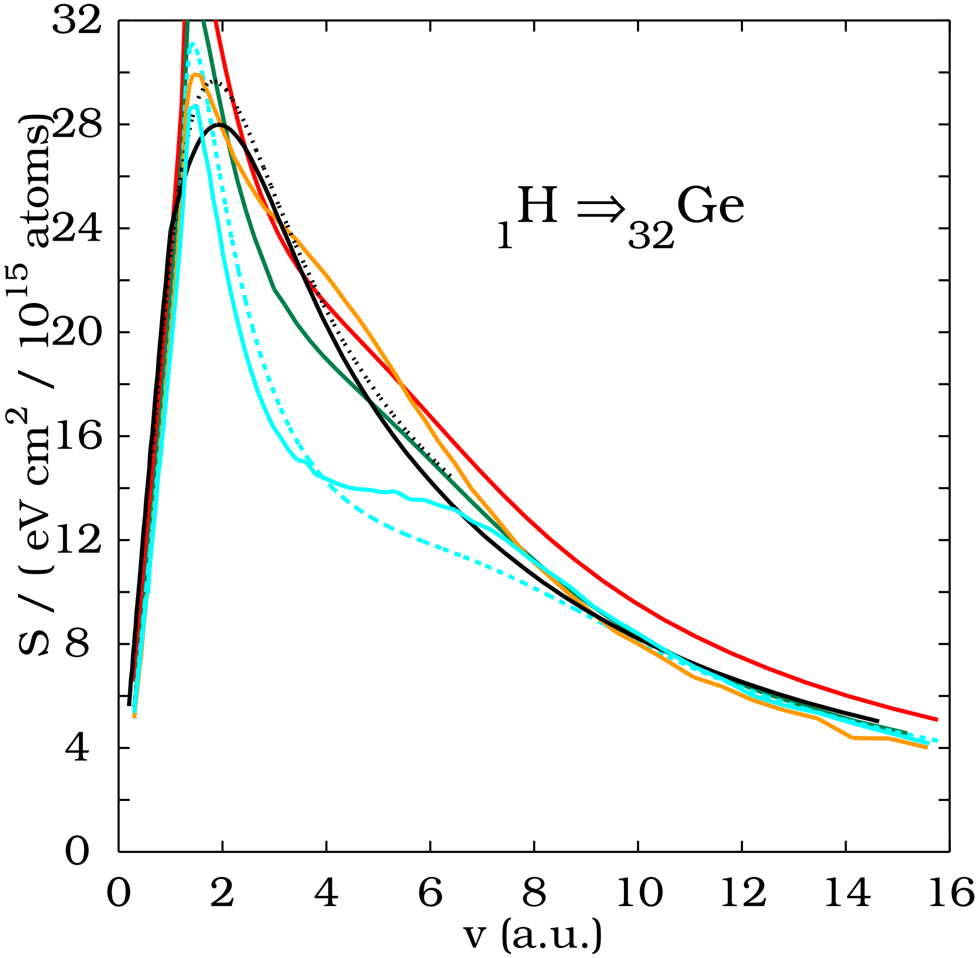

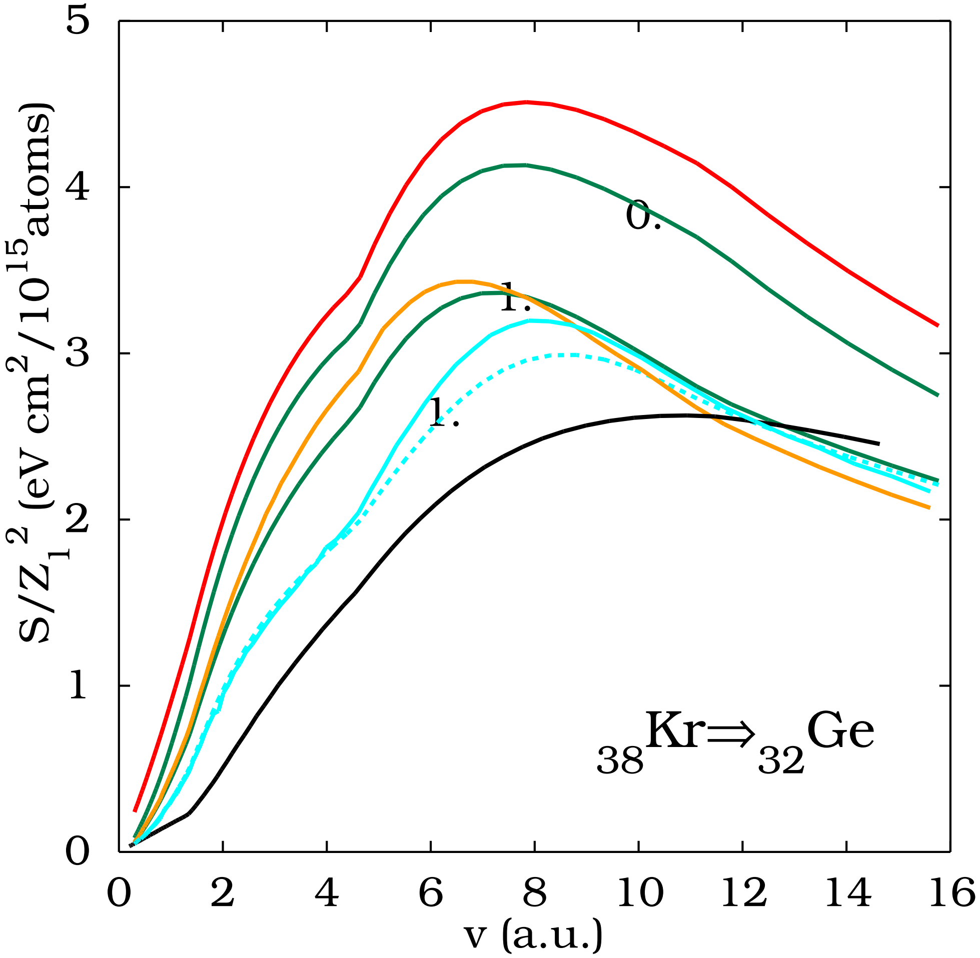

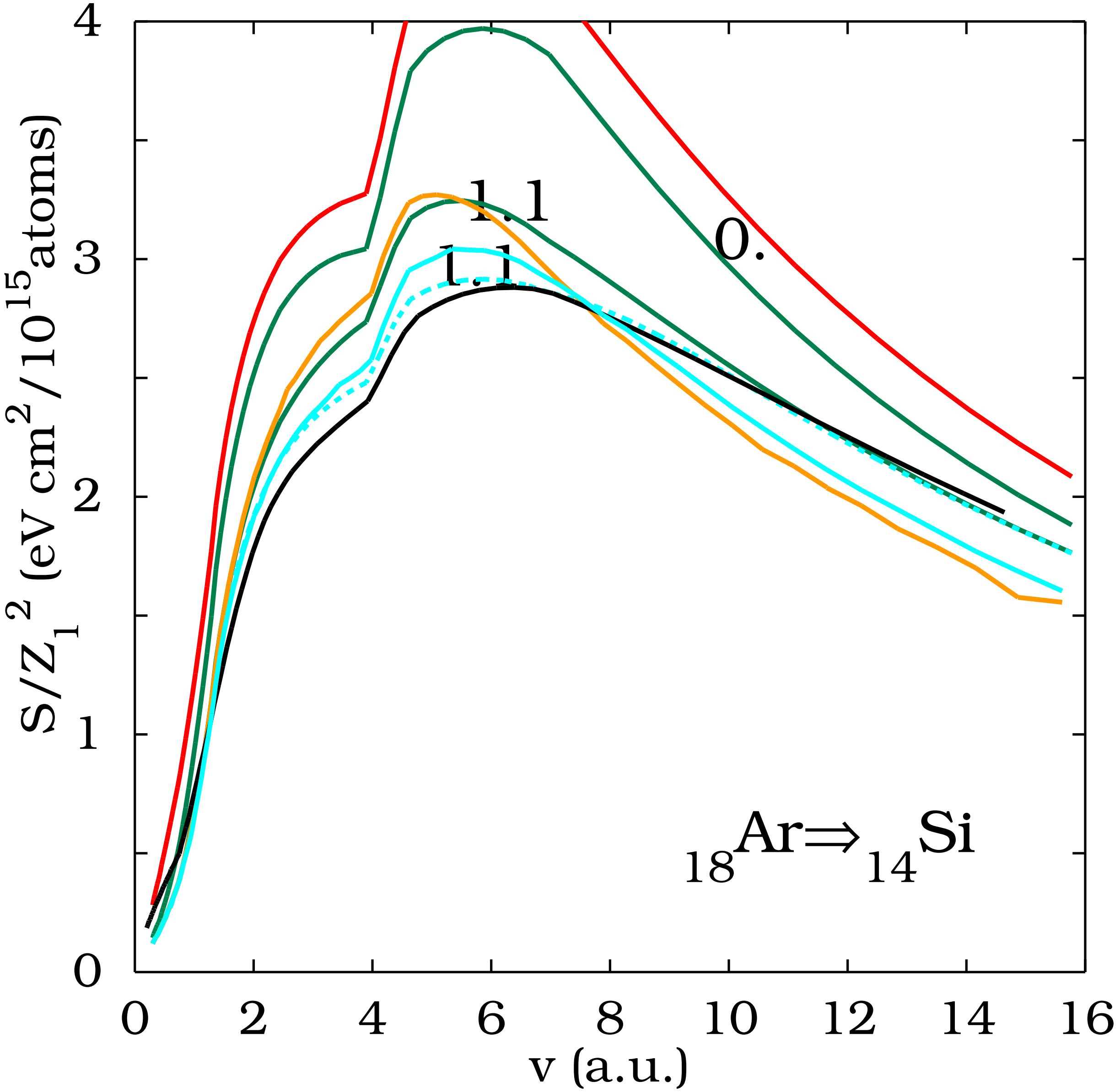

Summary:

The energy cut and dead sphere corrections reduce the electronic energy loss.

Geometric dilution of the susceptibilities and adding them instead of polarization charges shell by shell results in an increase at low and decrease at high ion velocities.

Non-Gaussian ground state distributions of *p* and *d* subshells shift the maximum of the electronic energy loss to higher velocities.